

# Research on Thermal Decomposition Kinetics and Thermal Safety for a New Epoxiconazole Crystal

Zhen-Yun Wei, Ji-Shuang Tan, Xiao-Hua Ma, Rong Kong, Xuan Liu, Chun-Sheng Cheng,\* and San-Xi Li\*



Cite This: *ACS Omega* 2021, 6, 5582–5590



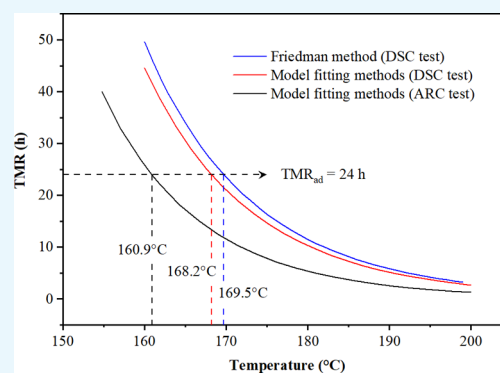
Read Online

ACCESS |

Metrics & More

Article Recommendations

**ABSTRACT:** To clarify the thermal safety inherent in a new epoxiconazole crystal, differential scanning calorimetry (DSC) and adiabatic accelerating rate calorimetry (ARC) were used for testing and research. The Friedman method and model method were used to analyze thermal decomposition kinetics based on the DSC data, and the *N*-order and autocatalytic decomposition reaction kinetic models were established. The double scan method was utilized to verify the autocatalytic effect during the decomposition process. The Friedman method, *N*-order, and autocatalytic model methods were used to study the substance's thermal decomposition characteristics. ARC data are utilized to verify the aforementioned prediction results and the kinetic parameters that were obtained based on ARC data from *N*-order and autocatalytic model methods that concur with the simulation results. This paper applies the *N*-order and autocatalytic model to the kinetic model to further predict thermal safety parameter time to maximum rate under adiabatic conditions.



## 1. INTRODUCTION

Epoxiconazole is a new, broad-spectrum, long-lasting triazole fungicide developed by Badische Anilin-und-Soda-Fabrik (BASF). It is effective on various pathogenic bacteria that affect crops, particularly cereals. In addition, epoxiconazole also possesses a certain regulation effect on the plant growth.<sup>1</sup> In recent years, epoxiconazole, as a triazole fungicide has seen a gradual increase in its market share around the world and maintains a high price, culminating in positive market prospects.

In addition, chemical accidents have been frequent, and most are the direct results of decomposition reactions.<sup>2</sup> As the international community focuses even more on safety in chemical production, thermal stabilities for substances have been clarified. Targeted measurements have been collected to avoid decomposition reactions, and accident causes have become increasingly important. Buser<sup>1,3</sup> et al. studied synthesizing and applying epoxiconazole with organic and inorganic peroxy acid,<sup>4</sup> chlorohydrin, alkyl hydrogen peroxide,<sup>5</sup> hydrogen peroxide, molecular oxygen,<sup>6</sup> and other as oxidants to epoxidate triazolene into epoxiconazole. However, no research from around the world has yet to report on the thermal stabilities for said substances. Most research into thermal stabilities for substances currently relies on a single calorimetry model and calculation method, and the results that have been obtained are biased.

New epoxiconazole crystals are obtained by recrystallization using commercial epoxiconazole by dichloroethane. We found that the fungicide efficacy of new epoxiconazole crystal was much higher than commercial epoxiconazole. In order to determine the thermal stability for the new epoxiconazole crystals, the differential scanning calorimetry (DSC) and accelerating rate calorimetry (ARC) with dynamic and adiabatic calorimetry models were used to test thermal decomposition characteristics. Using the AKTS software to process the DSC data based on the Friedman model and with the simulated isothermal DSC experiment, it was initially determined that an autocatalytic effect occurs during thermal decomposition of the new epoxiconazole crystal. So, a thermal explosion simulation was conducted. Meanwhile, TSS software was utilized to process DSC and ARC data based on the *N*-order and the autocatalytic model, and the thermal explosion simulation was conducted. Afterward, the double-scanning DSC experiments were utilized to verify the autocatalytic effect from epoxiconazole crystals throughout the thermal decomposition process. Finally, the forementioned three simulation

Received: December 9, 2020

Accepted: February 5, 2021

Published: February 16, 2021



results were compared and analyzed<sup>7</sup> to ensure the accuracy in the obtained data and provide a scientific basis for safe production, storage, and transportation for new epoxiconazole crystals.

## 2. RESULTS AND DISCUSSION

**2.1. Dynamic DSC Test Results and Analysis.** Thermal decomposition characteristics for new epoxiconazole crystals researched with dynamic DSC test exothermic peak heat-flow curve for epoxiconazole crystals under disparate temperature rise conditions are displayed in Figure 1, and dynamic DSC test exothermic peak data for the corresponding epoxiconazole crystal thermal decomposition reaction is displayed in Table 1.

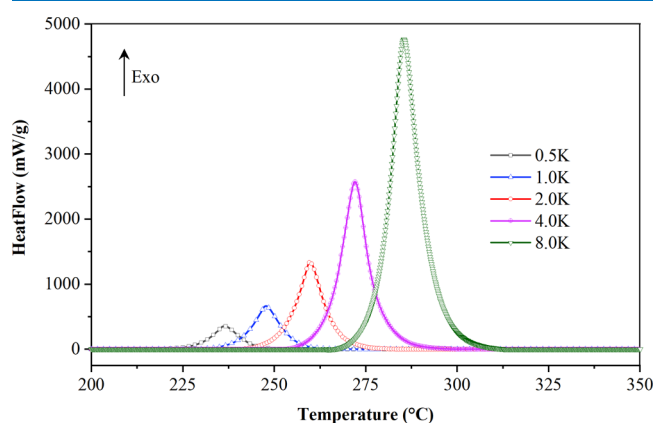


**Figure 1.** Dynamic DSC curves for new epoxiconazole crystals at scanning rates of 0.5, 1.0, 2.0, 4.0, and 8.0 K·min<sup>-1</sup>.

Figure 1 shows cases that under five different temperature rise rates, a clear exothermic peak appears when new epoxiconazole crystals undergo thermal decomposition. As the temperature rise rate increases, the exothermic peak drifts toward the high temperature area, which results in the initial decomposition temperature ( $T_{\text{onset}}$ ) and peak temperature ( $T_p$ ), gradually increasing with a sharper peak. It is more than likely that the new epoxiconazole crystals possess autocatalytic properties.<sup>2,8</sup> The induction period for the autocatalytic reaction causes a delay within the reaction process, resulting in no measurable exothermic reaction in the initial process. Any temperature rise can only be detected once the reaction rate has accelerated to a certain level post induction period. Afterward, acceleration behavior incited by an increase in the product concentration and temperature rise will become intense, and once it is out of control, the time to enact countermeasures will be insufficient.<sup>2</sup> Therefore, a deeper examination for the reaction is required.

Based on the analysis in Table 1, the initial decomposition temperature ( $T_0$ ) for new epoxiconazole crystals is 229.65–278.40 °C and the peak temperature ( $T_p$ ) is 236.37–285.49

°C. As the temperature rise rate increases, the decomposition reaction enthalpy changes, and its overall trend monotonically decreases. According to the relevant literature,<sup>9</sup> the reaction type can be preliminarily judged through observing changes in the reaction enthalpy trend ( $\Delta H$ ) for dynamic DSC testing under multiple groups of disparate temperature rise rates. If  $\Delta H$  changes with the temperature rise rate, the reaction type is most likely to be a competitive (parallel) type. Thus, it is preliminarily judged that the reaction type is a competitive (parallel) reaction. The average exothermic heat ( $\overline{\Delta H}$ ) from thermal decomposition of new epoxiconazole crystals across five tests is 404.66 kJ·kg<sup>-1</sup>.

**2.1.1. Differential Iso-Conversional Methods.** As displayed in Figure 2, activation energy  $E$ , linear correlation coefficient  $R$ , and  $\ln\{A_\alpha f(\alpha)\}$  the change curve for the reaction progress  $\alpha$  are obtained using the Friedman method within the iso-conversional differential method combined with the thermal decomposition curves at five disparate temperature rates.

As observed in Figure 2, the conversion rate range is  $\alpha = 0.05$ – $0.95$ .<sup>10</sup> The linear coefficient  $R$  remains constant between 0.99 and 1.00, and for all Arrhenius straight lines, the average linear correlation coefficient  $R = 0.9993$ , which indicates that the linear correlation sits at a high level. Between 0.05 and 0.95, the activation energy range for the new epoxiconazole crystal decomposition reaction is 105–136 kJ·mol<sup>-1</sup>, according to the Friedman differential method. The variations within the range are significant, which indicates that the decomposition reaction process is relatively complicated and cannot be employed in just one step;<sup>10,11</sup> meanwhile, the activation energy during the entire decomposition process is  $\geq 100$  kJ·mol<sup>-1</sup>. A higher activation energy means that the decomposition reaction is more sensitive to temperature.<sup>2</sup> The simulation curves, as shown in Figure 3a,b, are well in agreement with the experimental curves, indicating that the calculation results from the thermal decomposition kinetic constants  $E$  and  $\ln\{A_\alpha f(\alpha)\}$  are even more accurate.<sup>12</sup>

In chemical process safety, dynamic DSC is universally used for preliminary experimental screening in thermal risk assessments. Identifying autocatalytic reactions is important in terms of evaluating thermal risks. These reactions require our special attention and should be clearly distinguished from  $N$ -order reactions.<sup>8</sup> The most reliable method to currently identify autocatalytic decomposition reactions is to perform isothermal DSC and double-scan experiments. However, it is difficult to choose the appropriate experimental temperature throughout isothermal DSC experiments.<sup>2</sup> This paper presents an identification method for the autocatalytic decomposition reaction that is based on dynamic DSC. It utilizes the predictive isothermal experiment function in the AKTS software to analyze dynamic differential scanning experimental data to simulate isothermal DSC experiments at different temperatures. It can preliminarily judge whether an autocatalytic effect exists in a decomposition reaction based on peak

**Table 1.** Experimental Data for the Thermal Decomposition of New Crystals of Epoxiconazole by DSC Tests

| $\beta$ (K·min <sup>-1</sup> ) | mass (mg) | $T_{\text{onset}}$ (°C) | $T_p$ (°C) | $T_{\text{endset}}$ (°C) | $\Delta H$ (kJ·kg <sup>-1</sup> ) | $\overline{\Delta H}$ (kJ·kg <sup>-1</sup> ) | standard deviation (kJ·kg <sup>-1</sup> ) |
|--------------------------------|-----------|-------------------------|------------|--------------------------|-----------------------------------|--|---|
| 0.50                           | 4.09      | 229.57                  | 236.37     | 244.01                   | 427.56                            |  |   |
| 1.00                           | 4.15      | 241.09                  | 247.75     | 255.67                   | 407.08                            |  |   |
| 2.00                           | 4.15      | 253.38                  | 259.81     | 267.01                   | 406.50                            | 404.66                                       | 15.9                                      |
| 4.00                           | 4.11      | 264.39                  | 272.03     | 278.85                   | 398.61                            |  |   |
| 8.00                           | 4.17      | 278.40                  | 285.49     | 293.52                   | 383.56                            |  |   |

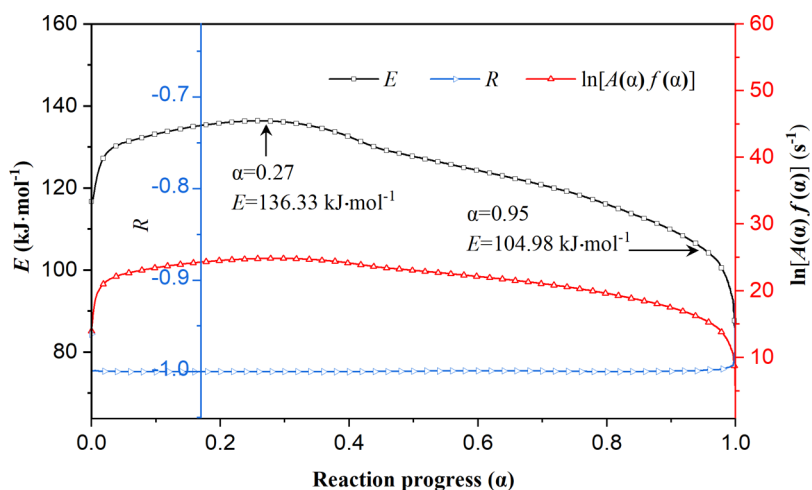


Figure 2. Curve of activation energy and decomposition reaction progress for new epoxiconazole crystals.

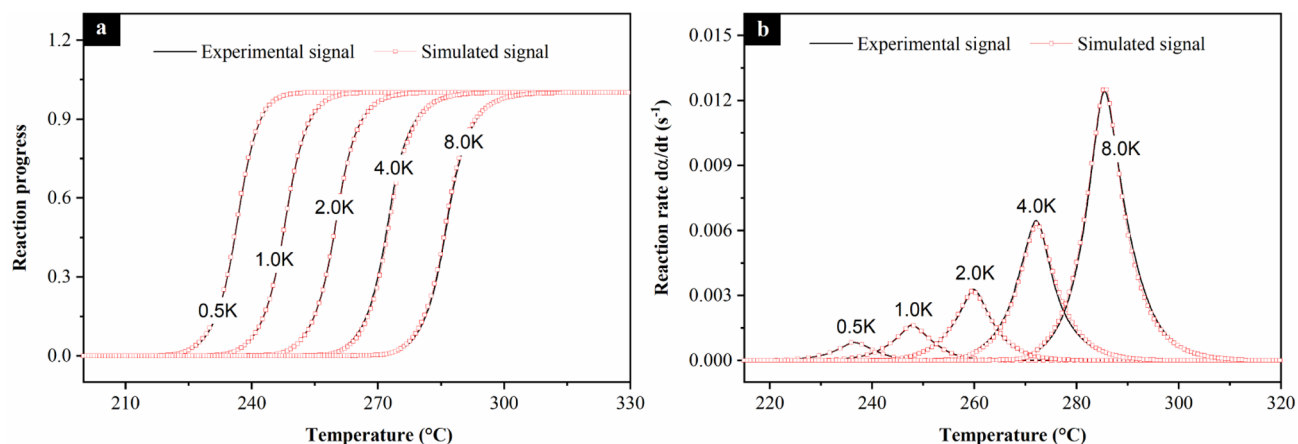


Figure 3. Curves of (a) reaction progress  $\alpha$  and (b) reaction rate  $d\alpha/dt$  with temperature at different heating rates.

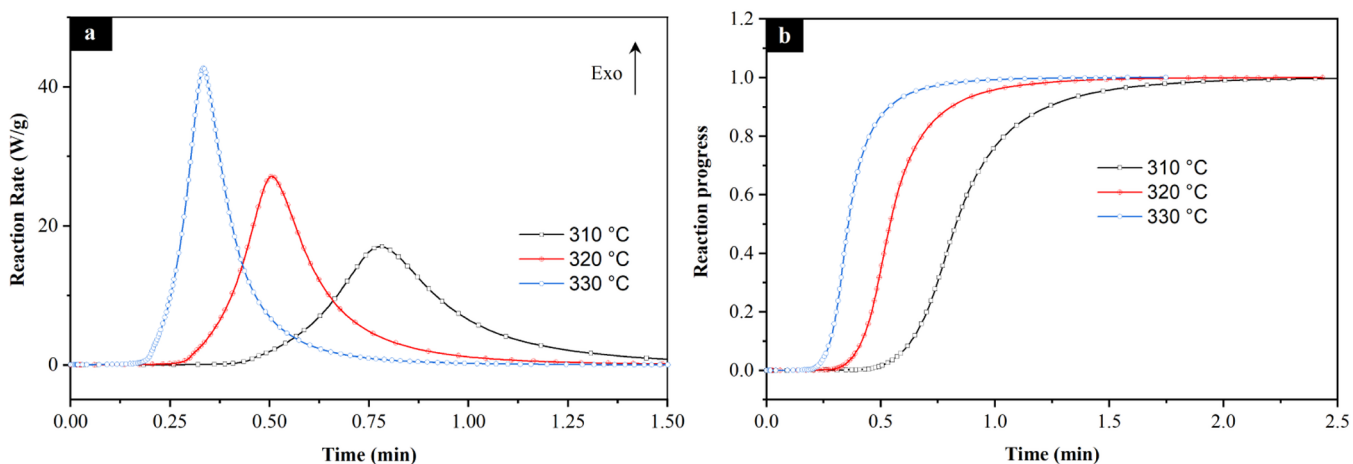


Figure 4. Curve of isothermal DSC experimental prediction results of new crystals of epoxiconazole. (a) Reaction rate curves and (b) reaction progress vs time.

shapes<sup>8</sup> and also provide a reference for selecting temperatures for DSC experiments.

To preliminarily determine whether an autocatalytic effect exists during new epoxiconazole crystal decomposition, the AKTS software prediction function is employed to predict isothermal DSC experiments at 310, 320, and 330 °C. The results are shown in Figure 4a,b.

It can be seen from Figure 4a,b that the decomposition reaction accelerates with time during the initial stage of epoxiconazole crystal decomposition. Once the reaction heat release rate reaches its maximum, it begins decreasing, and both a bell-shaped heat release rate curve and S-shaped conversion rate curve emerge, which concur with the results from isothermal DSC experiments reported in the literature.<sup>2,8</sup>

It shows that the autocatalytic effect may exist in the decomposition process for the new epoxiconazole crystal.

Once the kinetic parameters were determined with the iso-conversion differential method, the thermal phenomenon for the new epoxiconazole crystal under ideal adiabatic conditions continued to be simulated.<sup>10</sup> The simulated safety diagram is shown in Figure 5.

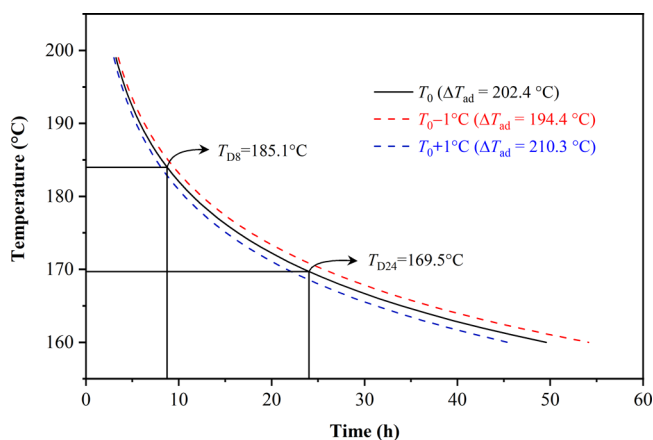


**Figure 5.** TMRad curve calculated from the kinetic parameters obtained from the DSC curve.

In Figure 5, it can be seen that under ideal adiabatic conditions ( $\Phi = 1$ ,  $\Delta H = 404.7 \pm 15.9 \text{ kJ}\cdot\text{kg}^{-1}$ ,  $C_p = 2.0 \text{ kJ}\cdot\text{kg}^{-1}$ , and  $\Delta T_{\text{ad}} = \Delta H/C_p\Phi = 202.4 \pm 8 \text{ }^\circ\text{C}$ ), which means that all heat released during decomposition in the sample is used to heat itself. When the maximum reaction arrives at times [time to maximum rate under adiabatic conditions (TMR<sub>ad</sub>)] is 8 and 24 h, the system temperatures for the epoxiconazole crystals are 185.1 °C ( $T_{D8}$ ) and 169.5 °C ( $T_{D24}$ ). In addition, Figure 5 shows us that the starting temperature significantly influences the adiabatic induction time (TMR<sub>ad</sub>) and adiabatic temperature rise ( $\Delta T_{\text{ad}}$ ).

**2.1.2. Model Fitting Methods.** The above analysis has led to the conclusion that the new crystal decomposition reaction of epoxiconazole is a complex two-step parallel reaction and possesses an autocatalytic effect. Therefore, employing TSS

software, a competitive  $N$ -order reaction and autocatalytic reaction model are utilized to describe the new epoxiconazole crystal thermal decomposition. The simulation results are displayed in Figure 6 and Table 2.

Figure 6 details that the degrees of fit between the experimental and simulated values are relatively high, the relative error is less than  $1 \times 10^{-6}$ , which indicates that employing the  $N$ -order reaction and autocatalytic reaction model is reliable when calculating the decomposition reaction kinetic parameters for new epoxiconazole crystals. Table 2 lists corresponding thermodynamic parameters, which can be explained through the two parallel stages below<sup>13</sup>

Step 1 ( $N$ -order reactions):  $A \rightarrow B$  (product 1)

$$r_1 = A_1 e^{-E_1/RT} (1 - \alpha)^n \quad (1)$$

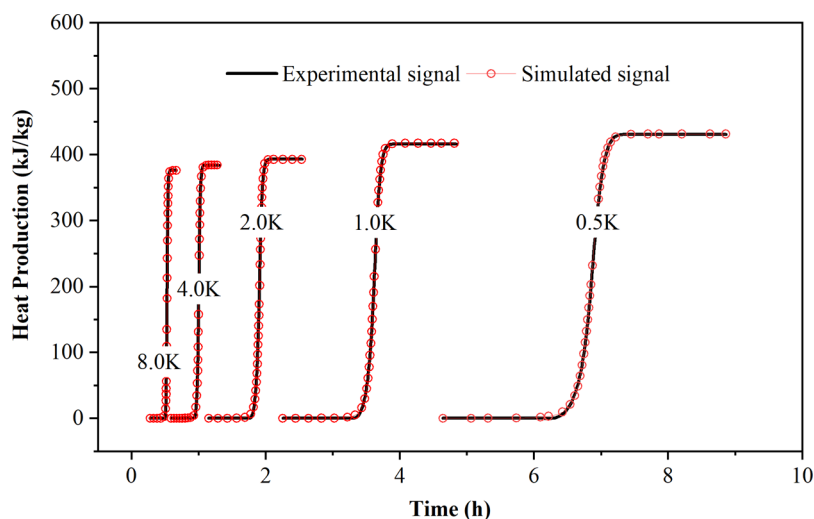
Step 2 (autocatalytic reaction)  $A \rightarrow C$  (product 2)

$$r_2 = A_2 e^{-E_2/RT} (1 - \alpha)^{n_1} (z_0 e^{-E_z/RT} + \alpha^{n_2}) \quad (2)$$

Formula:  $A$  refers to the pre-factor.  $E_1$  and  $E_2$  are the activation energy.  $n$ ,  $n_1$ , and  $n_2$  are reaction orders.  $R$  is the gas constant.  $T$  is the temperature.  $\alpha$  is the conversion rate of decomposition for the sample.  $z_0$  is the autocatalytic factor, and  $E_z$  is the composite value of activation energy.

The mathematical model uses the conversion rate ( $\alpha$ ) to obtain the main characteristics inherent in the epoxiconazole crystal decomposition reaction, such as the maximum reaction heat release rate, induction period, and so on. Thus, determining a reliable kinetic model is a better way to understand the autocatalysis phenomenon. This research has enabled us to predict runaway reaction parameters during the initial stage of the new epoxiconazole crystal life cycle, which ensures that the accident severity is reduced to a manageable level. This is, extremely significant to designing emergency measures.

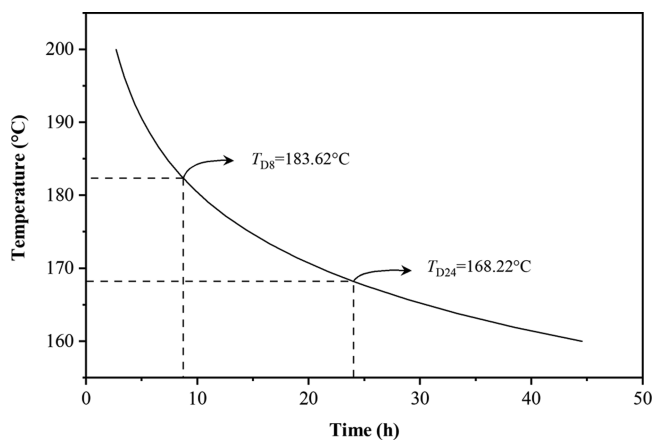
In Figure 7, it can be seen that under ideal adiabatic conditions ( $\Phi = 1$ ,  $\Delta H = 399.93 \text{ kJ}\cdot\text{kg}^{-1}$ ,  $C_p = 2.0 \text{ kJ}\cdot\text{kg}^{-1}$ ,  $\Delta T_{\text{ad}} = \Delta H/C_p\Phi = 199.97 \text{ }^\circ\text{C}$ ), which means that  $T_{D8}$  and  $T_{D24}$  are 183.62 °C and 168.22 °C, respectively. These results are consistent with the results obtained by the Friedman method in the equal conversion rate differentiation method ( $T_{D8}$  is 185.1 °C, and  $T_{D24}$  is 169.5 °C).



**Figure 6.** Comparison of experimental and simulation data for heat production with time of new crystals of epoxiconazole.

Table 2. Autocatalytic Reaction Kinetic Parameters Evaluation for New Crystals of Epoxiconazole at Different Scanning Rates

| parameters   | Nth    | autocatalytic reaction |        |        |        |        |
|--|--------|------------------------|--------|--------|--------|--------|
|  |        | 0.5 K                  | 1.0 K  | 2.0 K  | 4.0 K  | 8.0 K  |
| $\ln A$ [ $\ln(\text{s}^{-1})$ ]                         | 9.59   |                        |        | 22.72  |        |        |
| $E$ ( $\text{kJ}\cdot\text{mol}^{-1}$ )                  | 112.45 |                        |        | 119.81 |        |        |
| $n$  | 0.25   |                        |        |        |        |        |
| $n_1$  |        |                        |        | 1.08   |        |        |
| $n_2$  |        |                        |        | 1.01   |        |        |
| $\ln z_0$  |        |                        |        | -4.98  |        |        |
| $E_z$ ( $\text{kJ}\cdot\text{mol}^{-1}$ )                |        |                        |        | 8.59   |        |        |
| $\Delta H$ ( $\text{kJ}\cdot\text{kg}^{-1}$ )            | 10.29  | 431.01                 | 407.73 | 397.62 | 384.45 | 378.84 |
| $\overline{\Delta H}$ ( $\text{kJ}\cdot\text{kg}^{-1}$ ) |        |                        |        | 399.93 |        |        |

Figure 7.  $TMR_{ad}$  curve calculated from the kinetic parameters obtained from the DSC curve.

**2.1.3. Verification for the Autocatalytic Effect in Thermal Decomposition.** To verify new epoxiconazole crystal autocatalytic properties during the thermal decomposition process, DSC testing was conducted with the dual scan method. For substances with autocatalytic properties, even if a small part decomposes first, it will be accompanied by a sudden release of a significant amount of heat, which results in the DSC curves for said substances undergoing significant changes. Thus, this method is both rapid and reliable and can be used to identify autocatalytic behavior among substances.<sup>2</sup>

First, complete DSC testing was performed on new epoxiconazole crystals with a temperature rise rate of  $5.0 \text{ K}\cdot\text{min}^{-1}$  and a testing temperature range of  $30\text{--}350 \text{ }^\circ\text{C}$  to obtain the first DSC testing curve, which is recorded as A. Next, the new epoxiconazole crystals are heated to  $273 \text{ }^\circ\text{C}$  (near the initial decomposition temperature) at a temperature rise rate of  $5.0 \text{ K}\cdot\text{min}^{-1}$  under the same testing conditions. Then, the temperature was cooled to  $30 \text{ }^\circ\text{C}$  naturally, and once the instrument is stable, dynamic DSC testing was conducted with a temperature rise rate of  $5.0 \text{ K}\cdot\text{min}^{-1}$  and a testing temperature range of  $30\text{--}350 \text{ }^\circ\text{C}$  on the cooled sample to obtain the curve, which is recorded as B. The dynamic DSC experimental conditions and results from the dual-scanning method for new epoxiconazole crystals are shown in Table 3 and Figure 8, respectively.

By comparing Figure 8 and Table 3 with curve A, it can be seen that the initial decomposition temperature ( $T_0$ ), peak temperature ( $T_p$ ), and peak shape from the exothermic peak in curve B have all significantly changed. Both the initial decomposition temperature ( $T_0$ ) and peak temperature ( $T_p$ )

Table 3. Results of Dynamic DSC Experiments by the Double Scan Method

| DSC curve | mass (mg) | $T_{onset}$ ( $^\circ\text{C}$ ) | $T_{endset}$ ( $^\circ\text{C}$ ) | $T_p$ ( $^\circ\text{C}$ ) | $\Delta H$ ( $\text{kJ}\cdot\text{kg}^{-1}$ ) |
|-----------|-----------|----------------------------------|-----------------------------------|----------------------------|---|
| A         | 4.05      | 271.02                           | 284.38                            | 277.90                     | 400.37  |
| B         | 4.02      | 218.64                           | 283.35                            | 254.35                     | 235.02  |

moved in a lower direction in terms of temperature. The peak temperature  $T_p$  decreased by  $\Delta T = 23.55 \text{ }^\circ\text{C}$ , and the initial decomposition temperature  $T_0$  decreased by as much as  $52.38 \text{ }^\circ\text{C}$ . Because the samples in the double-scan experiment have been heated to the initial decomposition temperature, the sample has partially decomposed, and the decomposition product has a catalytic effect on new epoxiconazole crystal decomposition, moving the exothermic peak toward lower temperatures. This shows that an autocatalytic effect is present in the decomposition process that the sample underwent.

**2.2. ARC Test Results and Analysis.** Figure 9 shows the temperature–time curve and the temperature-rise rate–time curve for the exothermic phase of the new epoxiconazole crystals obtained from an adiabatic experiment. Relevant thermal decomposition parameters have been calculated and are listed in Table 4.

It can be seen in Figure 9 and Table 4 that under adiabatic conditions, the thermal decomposition inherent in epoxiconazole crystals begins at  $199.75 \text{ }^\circ\text{C}$  and reaches a maximum temperature rise rate of  $14.50 \text{ }^\circ\text{C}\cdot\text{min}^{-1}$  at 1.87 h (the corrected  $TMR_{ad}$  was 0.78 h). The final temperature was increased by  $94.65 \text{ }^\circ\text{C}$  (the adiabatic temperature rise  $\Delta T_{ad}$  in the sample after calibration was  $227.62 \text{ }^\circ\text{C}$ ), and the corrected specific reaction heat  $Q$  was  $454.32 \text{ kJ}\cdot\text{kg}^{-1}$ .

Once the decomposition reaction is triggered in the new epoxiconazole crystals, the temperature will rapidly rise, and the time is not sufficient to avoid an explosion. It is all too easy to lose control. These characteristics continue to indicate that a strong autocatalytic effect occurs in the decomposition process in the new epoxiconazole crystals.

To further clarify thermal decomposition characteristics inherent in new epoxiconazole crystals, the ARC data were imported into the aforementioned  $N$ -order reaction and autocatalytic reaction kinetic model to optimize and calculate the kinetic parameters. Figure 10 indicates the results from the experiment and kinetic fitting.

By analyzing the simulation results in Figure 10, it was found that the simulated data are relatively close to the experimental data, and the relative error is less than  $1 \times 10^{-6}$ , which indicates that the reaction kinetics calculated by the model is

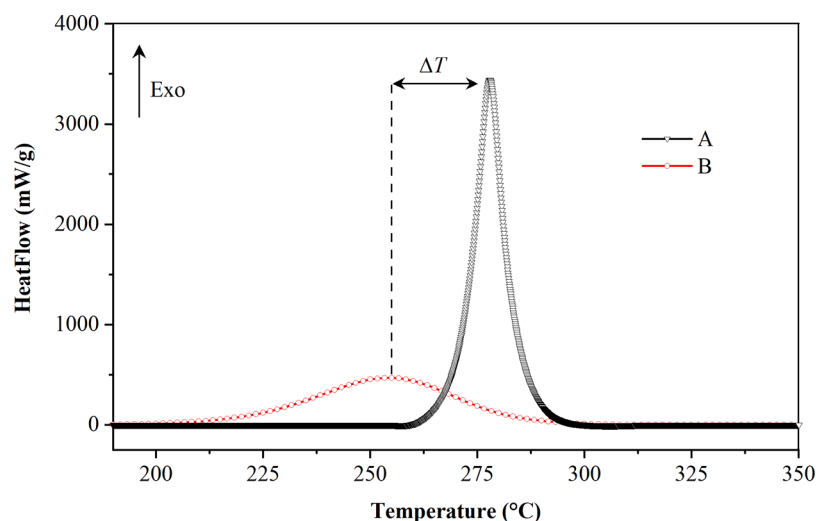


Figure 8. Dynamic DSC curve of the double-scanning method.

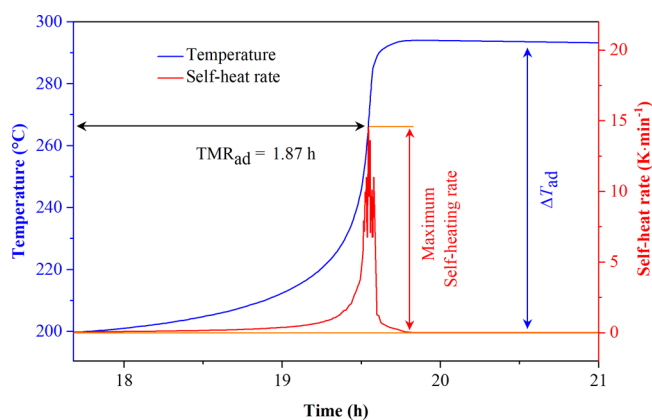


Figure 9. ARC test curve of the epoxiconazole dichloroethane crystal sample.

Table 4. ARC Analysis of New Crystals of Epoxiconazole

| sample   | dichloroethane crystals of epoxiconazole |
|--|--|
| total sample mass (g)                                | 3.54                                     |
| $C_p$ of sample ( $J \cdot g^{-1} \cdot K^{-1}$ )    | 2.00                                     |
| ARC cell mass (g)                                    | 22.61                                    |
| $C_p$ of ARC cell ( $J \cdot g^{-1} \cdot K^{-1}$ )  | 0.43                                     |
| set end temperature ( $^{\circ}C$ )                  | 300.00                                   |
| $\varphi$  | 2.37                                     |
| onset temperature ( $^{\circ}C$ )                    | 199.75                                   |
| final temperature ( $^{\circ}C$ )                    | 294.41                                   |
| max self-heating rate ( $^{\circ}C \cdot min^{-1}$ ) | 14.50                                    |
| time to maximum rate (h)                             | 1.87                                     |
| total heat ( $kJ \cdot kg^{-1}$ )                    | 454.32                                   |
| temperature rise ( $^{\circ}C$ )                     | 94.65                                    |

reliable. Table 5 shows the simulation kinetic parameters determined by TSS software combined with ARC data.

As shown in Figure 11 and Table 6, the kinetic parameters obtained from using different models for calorimeters and different kinetic models are in agreement. The predicted  $T_{D24}$  is between 160 and 170  $^{\circ}C$ , indicating that the kinetic data that were obtained by the thermokinetic method are reliable.

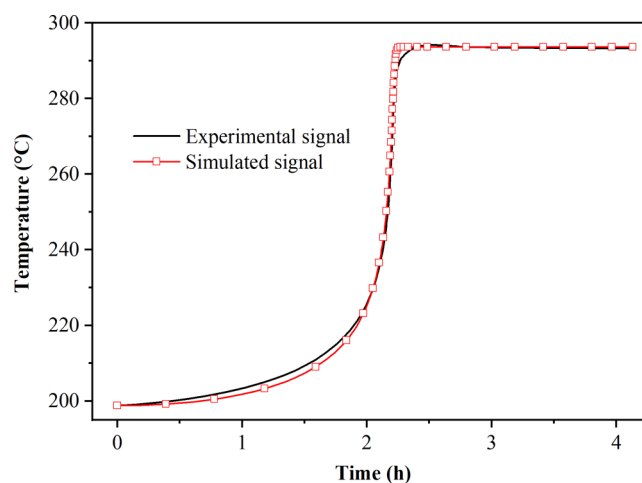


Figure 10. Simulated temperature versus time of new epoxiconazole crystals (ARC test).

Table 5. Kinetic Parameters of New Crystals of Epoxiconazole by  $N$ -Order and Autocatalytic Simulation of ARC Tests

| parameters                        | $N$ th | autocatalytic reaction |
|-----------------------------------|--------|------------------------|
| $\ln A$ [ $\ln(s^{-1})$ ]         | 8.32   | 24.54                  |
| $E$ ( $kJ \cdot mol^{-1}$ )       | 100.33 | 132.22                 |
| $n$                               | 1.33   |                        |
| $n_1$                             |        | 0.95                   |
| $n_2$                             |        | 0.52                   |
| $\ln z_0$                         |        | -5.06                  |
| $E_z$ ( $kJ \cdot mol^{-1}$ )     |        | 19.59                  |
| $\Delta H$ ( $kJ \cdot kg^{-1}$ ) | 8.76   | 447.24                 |

### 3. CONCLUSIONS

By using DSC and ARC under dynamic and adiabatic conditions to test the thermal decomposition characteristics inherent in new epoxiconazole crystals and kinetic simulations, the results indicate several things: the new epoxiconazole crystal follows the  $N$ -order and autocatalytic model decomposition reaction kinetic model during the decomposition process, and the initial decomposition temperature is 199.97

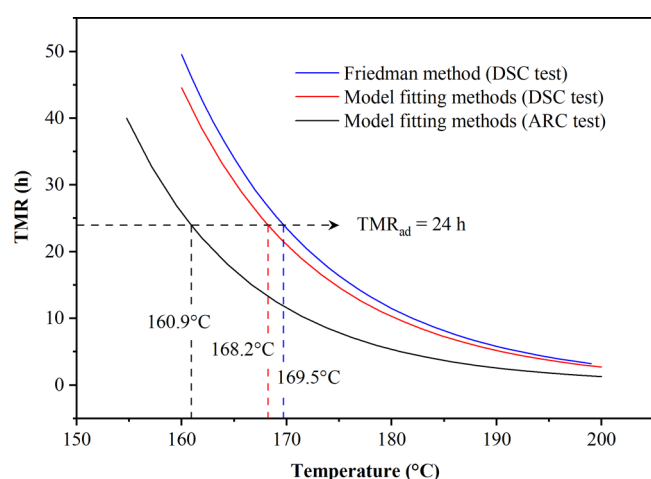


Figure 11. Comparison of TMR curves obtained by three methods.

The chemical structure is:

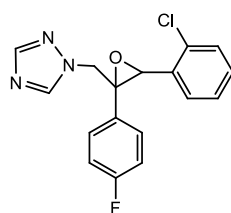


Figure 12. Epoxiconazole molecular structure.

Table 6.  $T_{D8}$  and  $T_{D24}$  Obtained by Friedman Method (DSC Test),  $N$  Order and Autocatalytic Model Method (DSC Test), and  $N$  Order and Autocatalytic Model Method (ARC Test)

| parameters | Friedman method (DSC test) (°C) | model fitting methods (DSC test) (°C) | model fitting methods (ARC test) (°C) |
|------------|---------------------------------|---------------------------------------|---------------------------------------|
| $T_{D8}$   | 185.2                           | 183.5                                 | 174.6                                 |
| $T_{D24}$  | 169.5                           | 168.2                                 | 160.9                                 |

°C. The exothermic heat is 454.32 kJ·kg<sup>-1</sup>, and the rise in adiabatic temperature is 94.65 °C (the adiabatic temperature rise  $\Delta T_{ad}$  in the sample after calibration was 227.62 °C).  $TMR_{ad}$  is 1.87 h at 199.97 °C (the corrected  $TMR_{ad}$  was 0.78 h), and the corresponding temperature of  $TMR_{ad}$  at 24 h is 160.9 °C. Once the decomposition reaction occurs, it is not easily controlled, so it is not advisable to have temperatures exceed 160.9 °C in the product and use processes. In follow-ups, we will continue to explore the disparities among new epoxiconazole crystals, the original epoxiconazole drug, and other types of crystals, and the influences different crystals have on thermal safety samples.

## 4. EXPERIMENTS AND METHODS

**4.1. Samples.** New epoxiconazole crystal was obtained upon dissolving commercial epoxiconazole in dichloroethane. The solution was heating and cooling at different rates. The obtained suspension was filtered and dried to give epoxiconazole (purity 99%).

**4.2. Differential Scanning Calorimetry.** The heat-flow differential scanning calorimeter (DSC-1) utilized in the experiment was produced by Mettler Toledo, Switzerland, with a calorimetric sensitivity of 0.04  $\mu$ W. The sample cell and reference cell are both 25  $\mu$ L high-pressure of 25 MPa gold-

plated crucibles. Sample masses were 3–5 mg in a nitrogen atmosphere, and the test temperature range was 30–350 °C and a dynamic heating rate ( $\beta$ ) was 0.5, 1.0, 2.0, 4.0, and 8.0 K·min<sup>-1</sup>.

**4.3. Accelerating Rate Calorimetry.** The model for the adiabatic accelerating rate calorimeter used in the test is PhITEC I produced by the British Company HEL, and the sensitivity for heat release detection is 0.02 °C·min<sup>-1</sup>. The sample cell is a Hastelloy spherical test cell with a 10 mL volume, a 20 MPa upper pressure limit, and a room temperature to 500 °C test temperature range. The experimental test sample mass is about 3.5, and the temperature rise step is 5 °C. 130–300 °C is the experimental rise step and under a nitrogen atmosphere. The temperature rises linearly from room temperature to 130 °C and runs in the heating-wait-search mode at 130–300 °C.

**4.4. Thermal Decomposition Kinetic Parameter Calculation Method.** **4.4.1. Differential Iso-Conversional Methods.** The Friedman method is the most common method for the differential iso-conversional method and is used to determine kinetic parameters in the AKTS software. This method is based on the Arrhenius equation. With the condition that the reaction conversion rate  $\alpha$  remains unchanged, the reaction rate is merely a function of temperature. During the entire reaction process, both activation energy  $E$  and pre-exponential factor  $A$  are functions of  $\alpha$ .<sup>9,14</sup>

$$\beta \frac{d\alpha}{dt} = \{A_{\alpha} f(\alpha)\} \exp\left(-\frac{E_{\alpha}}{RT(t_{\alpha})}\right) \quad (3)$$

Finding the logarithm on both sides of the equation obtains the differential equation

$$\ln\left(\beta \frac{d\alpha}{dt}\right) = \ln\{A_{\alpha} f(\alpha)\} - \frac{E_{\alpha}}{R} \frac{1}{T(t_{\alpha})} \quad (4)$$

where  $\beta$ ,  $t_{\alpha}$ ,  $T(t_{\alpha})$ ,  $E_{\alpha}$  and  $A_{\alpha}$  are the heating rate, time, temperature, apparent activation energy, and preexponential factor, at conversion  $\alpha$ , respectively, and  $-E_{\alpha}/R$  and  $\ln\{A_{\alpha} f(\alpha)\}$  are the slope and the intercept with the vertical axis of plot of  $\ln(d\alpha/dt)$  versus  $1/T(t_{\alpha})$ .

To describe the kinetic process, the differential iso-conversional method employs multiple single-step kinetic equations, and pre-exponential factors and activation energy in the equations are not considered constants anymore but conversion functions. Each equation possesses a certain conversion rate degree, which is related to the temperature range that is then related to the conversion rate. This method is ultimately used for the mechanism and kinetic analysis as well as reliable kinetic prediction.<sup>2,10</sup>

**4.4.2. Model Fitting Methods.** The equal conversion rate differential method cannot provide any information on the reaction mechanism, particularly for more complex reactions. Distinguishing between  $N$ -order reactions and autocatalytic reactions is challenging.<sup>15</sup> Thus, TSS software is employed with a kinetic model fitting method for nonlinear fitting to determine the reaction kinetic model.<sup>16</sup> This method initially postulates that the conversion rate for the reaction system is composed of one or more variable sets from the nonlinear reaction equation. The simulated response curve can be obtained through substitutions in the reaction equation and variable adjustments in the equation, which cause the curve to

gradually approach the true response curve. When fitting the curve to the data from the experiment, the variables are currently kinetic parameters from the reaction. By simplifying the reaction kinetic model, though no detailed descriptions for the reaction mechanism exist, the main reaction characteristics can be appropriately expressed. In practice, it is commonly utilized in process safety research.<sup>17</sup>

## AUTHOR INFORMATION

### Corresponding Authors

**Chun-Sheng Cheng** – Key Laboratory of Polymer and Catalyst Synthesis Technology of Liaoning Province, School of Environmental and Chemical Engineering, Shenyang University of Technology, Shenyang 110870, Liaoning, China; Chemical Industry Safety Technology & Engineering Center, Shenyang Research Institute of Chemical Industry, Shenyang 110021, Liaoning, China; [orcid.org/0000-0001-7185-7560](https://orcid.org/0000-0001-7185-7560); Email: [chengchunsheng@sinochem.com](mailto:chengchunsheng@sinochem.com)

**San-Xi Li** – Key Laboratory of Polymer and Catalyst Synthesis Technology of Liaoning Province, School of Environmental and Chemical Engineering, Shenyang University of Technology, Shenyang 110870, Liaoning, China; Email: [lisx@sut.edu.cn](mailto:lisx@sut.edu.cn)

### Authors

**Zhen-Yun Wei** – School of Material Science and Engineering, Shenyang University of Technology, Shenyang 110870, Liaoning, China; Chemical Industry Safety Technology & Engineering Center, Shenyang Research Institute of Chemical Industry, Shenyang 110021, Liaoning, China

**Ji-Shuang Tan** – Chemical Industry Safety Technology & Engineering Center, Shenyang Research Institute of Chemical Industry, Shenyang 110021, Liaoning, China

**Xiao-Hua Ma** – School of Material Science and Engineering, Shenyang University of Technology, Shenyang 110870, Liaoning, China; Chemical Industry Safety Technology & Engineering Center, Shenyang Research Institute of Chemical Industry, Shenyang 110021, Liaoning, China

**Rong Kong** – Chemical Industry Safety Technology & Engineering Center, Shenyang Research Institute of Chemical Industry, Shenyang 110021, Liaoning, China

**Xuan Liu** – Chemical Industry Safety Technology & Engineering Center, Shenyang Research Institute of Chemical Industry, Shenyang 110021, Liaoning, China

Complete contact information is available at:

<https://pubs.acs.org/10.1021/acsomega.0c05988>

### Author Contributions

Z.-Y.W.: Conceptualization, methodology, validation, supervision, and writing—original draft. J.-S.T.: Experiment, data curation, and software. X.-H.M., R.K., and X.L.: Data curation and software. C.-S.C.: Writing—review and editing. S.-X.L.: Investigation and supervision.

### Notes

The authors declare no competing financial interest.

## ACKNOWLEDGMENTS

The authors are grateful for financial support from the Science and Technology Major Project of Liaoning Province (2019), China (project no. 2019JH1/10300002).

## ABBREVIATIONS

|                             |  |
|-----------------------------|--|
| $\beta$                     | dynamic heating rate [ $\text{K}\cdot\text{min}^{-1}$ ]  |
| $T_{\text{onset}}$          | onset temperature [ $^{\circ}\text{C}$ ]   |
| $T_{\text{endset}}$         | endset temperature [ $^{\circ}\text{C}$ ]  |
| $T_{\text{p}}$              | peak temperature [ $^{\circ}\text{C}$ ]  |
| $E_{\text{a}}$              | activation energy [ $\text{J}\cdot\text{mol}^{-1}$ ]   |
| $m_{\text{cell}}$           | ARC cell mass [g]  |
| $m_{\text{r}}$              | total sample mass [g]  |
| $C'_{\text{p}}$             | specific heat capacity of the cell [ $\text{J}\cdot\text{g}^{-1}\cdot\text{K}^{-1}$ ]                    |
| $C'_{\text{p,cell}}$        | specific heat capacity of the sample [ $\text{J}\cdot\text{g}^{-1}\cdot\text{K}^{-1}$ ]                  |
| $\Delta H$                  | reaction enthalpy [ $\text{kJ}\cdot\text{kg}^{-1}$ ]   |
| $\frac{\Delta H}{\Delta T}$ | average reaction enthalpy [ $\text{kJ}\cdot\text{kg}^{-1}$ ]   |
| $\Delta T_{\text{ad}}$      | adiabatic temperature rise [ $^{\circ}\text{C}$ ]  |
| $\text{TMR}_{\text{ad}}$    | time to maximum rate under adiabatic conditions [h]  |
| $T_{\text{D}8}$             | initial process temperature at which $\text{TMR}_{\text{ad}}$ is 8 h [ $^{\circ}\text{C}$ ]              |
| $T_{\text{D}24}$            | initial process temperature at which $\text{TMR}_{\text{ad}} = 24$ h [ $^{\circ}\text{C}$ ]              |
| $\Phi$                      | thermal inertia factor; $\Phi = 1 + \frac{m_{\text{cell}}C'_{\text{p,cell}}}{m_{\text{r}}C'_{\text{p}}}$ |

## REFERENCES

- (1) Burger, T.; Karbach, S.; Niemeyer, J.; Schlecker, R. Synthesis of four  $^{14}\text{C}$ -isotopomers of epoxiconazole, a new triazole fungicide. *J. Labelled Compd. Radiopharm.* **1996**, *38*, 173–178.
- (2) *Thermal Safety of Chemical Processes: Risk Assessment and Process Design*, 2nd; Stoessel, F., Ed.; Wiley-VCH, 2020.
- (3) Buerge, I. J.; Poiger, T.; Müller, M. D.; Buser, H.-R. Influence of pH on the stereoselective degradation of the fungicides epoxiconazole and cyproconazole in soils. *Environ. Sci. Technol.* **2006**, *40*, 5443–5450.
- (4) Klein, S.; Roberts, S. M. 2-Substituted-2,4-endo-dimethyl-8-oxabicyclo[3.2.1]octan-3-ones as catalysts for the asymmetric epoxidation of some alkenes with Oxone. *J. Chem. Soc., Perkin Trans. 1* **2002**, 2686–2691.
- (5) Page, P. C. B.; Buckley, B. R.; Heaney, H.; Blacker, A. J. Asymmetric epoxidation of cis-alkenes mediated by iminium salts: highly enantioselective synthesis of levromakalim. *Org. Lett.* **2005**, *7*, 375–377.
- (6) Hayashi, T.; Tanaka, K.; Haruta, M. Selective Vapor-Phase Epoxidation of Propylene over Au/TiO<sub>2</sub>Catalysts in the Presence of Oxygen and Hydrogen. *J. Catal.* **1998**, *178*, 566–575.
- (7) Leonhardt, J.; Hugo, P. Comparison of thermokinetic data obtained by isothermal, isoperibolic, adiabatic and temperature programmed measurements. *J. Therm. Anal.* **1997**, *49*, 1535–1551.
- (8) Bou-Diab, L.; Fierz, H. Autocatalytic decomposition reactions, hazards and detection. *J. Hazard. Mater.* **2002**, *93*, 137–146.
- (9) Moukhina, E. Determination of kinetic mechanisms for reactions measured with thermoanalytical instruments. *J. Therm. Anal. Calorim.* **2012**, *109*, 1203–1214.
- (10) Vyazovkin, S.; Burnham, A. K.; Criado, J. M.; Pérez-Maqueda, L. A.; Popescu, C.; Sbirrazzuoli, N. ICTAC Kinetics Committee recommendations for performing kinetic computations on thermal analysis data. *Thermochim. Acta* **2011**, *520*, 1–19.
- (11) Ma, X.-H.; Tan, J.-S.; Wei, Z.-Y.; Kong, R.; Li, Q.-G.; Li, S.-X.; Cheng, C.-S. Thermal safety study of (5,6-(dicarboxylate)-pyridin-3-yl) methyl-trimethyl ammonium bromide based on decomposition kinetics. *J. Therm. Anal. Calorim.* **2020**, DOI: 10.1007/s10973-020-09755-z.
- (12) Jia, M.; Guo, S.; Gao, S.; Wang, Q.; Sun, J. Thermal decomposition mechanism of diisopropyl azodicarboxylate and its thermal hazard assessment. *Thermochim. Acta* **2020**, *688*, 178601.
- (13) Das, M.; Shu, C.-M. A green approach towards adoption of chemical reaction model on 2,5-dimethyl-2,5-di-(tert-butylperoxy)-hexane decomposition by differential isoconversional kinetic analysis. *J. Hazard. Mater.* **2016**, *301*, 222–232.

(14) Roduit, B.; Folly, P.; Berger, B.; Mathieu, J.; Sarbach, A.; Andres, H.; Ramin, M.; Vogelsanger, B. Evaluating sadt by advanced kinetics-based simulation approach. *J. Therm. Anal.* **2008**, *93*, 153–161.

(15) Wang, S.-Y.; Kossoy, A. A.; Yao, Y.-D.; Chen, L.-P.; Chen, W.-H. Kinetics-based simulation approach to evaluate thermal hazards of benzaldehyde oxime by DSC tests. *Thermochim. Acta* **2017**, *655*, 319–325.

(16) Opfermann, J. Kinetic Analysis Using Multivariate Non-linear Regression. *J. Therm. Anal. Calorim.* **2000**, *60*, 641–658.

(17) Cao, C.-R.; Liu, S.-H.; Chi, J.-H.; I, Y.-P.; Shu, C.-M. Using thermal analysis and kinetics calculation method to assess the thermal stability of azobisdimethylvaleronitrile. *J. Therm. Anal. Calorim.* **2019**, *138*, 2853–2863.